Published in final edited form as:
Science. 2012 September 28; 337(6102): 1668–1672. doi:10.1126/science.1224947.

Sedlin Controls the ER Export of Procollagen by Regulating the Sar1 Cycle

Rossella Venditti[1,*], **Tiziana Scanu**[2,*,†], **Michele Santoro**[1], **Giuseppe Di Tullio**[2], **Alexander Spaar**[2], **Renato Gaibisso**[2], **Galina V. Beznoussenko**[2,†], **Alexander A. Mironov**[2,‡], **Alexander Mironov Jr.**[2,§], **Leopoldo Zelante**[3], **Maria Rosaria Piemontese**[3], **Angelo Notarangelo**[3], **Vivek Malhotra**[4,5], **Barbara M. Vertel**[6], **Cathal Wilson**[1], and **Maria Antonietta De Matteis**[1,‖]

[1]Telethon Institute of Genetics and Medicine, Via Pietro Castellino 111, Naples 80131, Italy

[2]Consorzio Mario Negri Sud, Via Nazionale, Santa Maria Imbaro (Chieti) 66030, Italy

[3]Medical Genetics Unit, IRCCS Casa Sollievo della Sofferenza, 71013 San Giovanni Rotondo, Foggia, Italy

[4]Department of Cell and Developmental Biology, Centre de Regulacio Genomica, 08010 Barcelona, Spain

[5]Institució Catalana de Recerca i Estudis Avançats, Pg. Lluis Companys 23, 08010 Barcelona, Spain

[6]Department of Cell Biology and Anatomy, Rosalind Franklin University of Medicine and Science, North Chicago, IL 60064, USA

Abstract

Newly synthesized proteins exit the endoplasmic reticulum (ER) via coat protein complex II (COPII) vesicles. Procollagen (PC), however, forms prefibrils that are too large to fit into typical COPII vesicles; PC thus needs large transport carriers, which we term megacarriers. TANGO1 assists PC packing, but its role in promoting the growth of megacarriers is not known. We found that TANGO1 recruited Sedlin, a TRAPP component that is defective in spondyloepiphyseal dysplasia tarda (SEDT), and that Sedlin was required for the ER export of PC. Sedlin bound and promoted efficient cycling of Sar1, a guanosine triphosphatase that can constrict membranes, and thus allowed nascent carriers to grow and incorporate PC prefibrils. This joint action of TANGO1 and Sedlin sustained the ER export of PC, and its derangement may explain the defective chondrogenesis underlying SEDT.

Newly synthesized protein cargoes are exported from the endoplasmic reticulum (ER) in transport carriers. Cargo sorting and carrier budding occur at ER exit sites (ERES) and are mediated by the small guanosine triphosphatase (GTPase) Sar1, which recruits the COPII coat complex (1). Procollagen (PC), however, forms 300-nm triple helices whose size exceeds that of typical 60- to 90-nm COPII vesicles. Although there has been important progress in identifying receptors such as TANGO1 that guide the packing of PCs into COPII transport carriers (2-4), the growth promotion mechanism of such megacarriers is unknown,

‖To whom correspondence should be addressed. dematteis@tigem.it.
*These authors contributed equally to this work.
†Present address: Division of Cell Biology, Netherlands Cancer Institute, Plesmanlaan 121, 1066 CX Amsterdam, Netherlands.
‡Present address: IFOM-IEO Campus, Via Adamello, 20139 Milan, Italy.
§Present address: Faculty of Life Sciences, University of Manchester, Manchester M13 9PT, UK.

Supplementary Materials
www.sciencemag.org/cgi/content/full/337/6102/1668/DC1 Materials and Methods, Figs. S1 to S13, Table S1, References (21-38)

Europe PMC Funders Author Manuscripts

as is the nature of the timer that delays fission of the nascent carriers until they reach an adequate size.

Spondyloepiphyseal dysplasia tarda (SEDT) is an X-linked skeletal disorder characterized by short stature, a short trunk, and precocious osteoarthritis. SEDT is caused by mutations in the gene *SEDL* (5); the underlying defect is a derangement in chondrogenesis reflecting the inability of chondrocytes to properly secrete extracellular matrix components (6). Sedlin, the *SEDL* product, is a component of a highly conserved multisubunit complex, TRAPP, which functions at various steps in intracellular transport (7), but the role of Sedlin (also called TRAPPC2) in these processes remains unknown.

The observations that a defect in Sedlin leads to cartilage-restricted consequences, and that there are shared clinical signs between patients with some mutations of type II PC (PCII) (8, 9) and Sedlin (5), prompted us to examine the impact of Sedlin knockdown (KD) (fig. S1) on trafficking of PCII in chondrocytes (10) and, in comparison, on trafficking of a reporter cargo, the temperature-sensitive variant of vesicular stomatitis virus G protein (ts045–VSV-G). The transport of PCII and VSV-G along the secretory pathway was synchronized by incubating cells at 40°C, resulting in reversible misfolding and ER retention of both cargoes, and then shifting the cells to 32°C to release the ER block (11). PCII transport was impaired by Sedlin depletion, with a marked inhibition of its ER exit (Fig. 1, A and B, and fig. S2A) and extracellular secretion (Fig. 1C). This impairment was partially rescued by expression of an RNA-resistant form of Sedlin (Fig. 1B). By contrast, transport of newly synthesized VSV-G was indistinguishable in Sedlin-depleted cells relative to control cells (Fig. 1, A and B, and fig. S2B). Sedlin KD did not appreciably affect total protein secretion (Fig. 1D). We extended our analysis to the transport of other cargoes, including type I PC (PCI), CD8α (Fig. 1E), albumin, and α1-antitrypsin. (Fig. 1F). PCI was the only cargo whose ER exit was affected by Sedlin depletion. All other cargoes examined exited the ER and reached the plasma membrane at apparently normal rates. Sedlin plays its role in PC trafficking as a TRAPP component, because a similar selective impairment of the ER exit of PC was induced by depleting the whole TRAPP by knockdown of Bet3 (TRAPPC3), a core component of the complex that, when depleted, destabilizes TRAPP (12) (fig. S1A and figs. S3 to S5). We then analyzed fibroblasts from SEDT patients (fig. S6). During the 40°C block, mCherry-PCII was retained in the ER in both wild-type and SEDTcells. After 30 min at 32°C, mCherry-PCII was almost completely concentrated in the Golgi complex in wild-type cells but remained in the ER in SEDT cells (Fig. 1G and fig. S6). Expression of wild-type Sedlin in SEDT fibroblasts partially rescued the ER export of mCherry-PCII (Fig. 1G).

The requirement of Sedlin for the ER exit of PC suggested that it might play a role at the ERES. Indeed, Sedlin associated with ERES (Fig. 2A), as shown for Bet3 (7). Sedlin was massively recruited to ERES during a synchronized wave of PCII transport (Fig. 2, B and C). We wondered how Sedlin, a cytosolic protein, could sense the presence of PC in the ER lumen. Because the transmembrane protein TANGO1 is a PC receptor at ERES (2, 3), we investigated whether recruitment of Sedlin to ERES involved TANGO1. TANGO1 overexpression increased Sedlin association with ERES (Fig. 2D) and also accelerated the ER exit of PC (fig. S7). Conversely, TANGO1 depletion (fig. S1B) decreased Sedlin association with ERES (Fig. 2E). We next explored the molecular mechanisms underlying TANGO1-mediated recruitment of Sedlin to the ERES and found that Sedlin and TANGO1 physically interacted (Fig. 2F).

The above findings prompted us to investigate the role of Sedlin at ERES. Sedlin depletion slowed the COPII coat cycle because it prolonged the recovery time of green fluorescent protein (GFP)–tagged Sec23 fluorescence recovery after photobleaching (FRAP) (Fig. 2G) and slowed the dissociation of GFP-Sec23 from ERES membranes, as assessed by

fluorescence loss in photobleaching [dissociation rate (K_{off}) values, 0.032 s^{-1} in control cells, 0.022 s^{-1} in Sedlin KD cells]. GFP-Sec23 exhibited slower dynamics in SEDT fibroblasts relative to wild-type fibroblasts as well, and the expression of wild-type Sedlin in SEDT fibroblasts rescued the COPII cycling defect (Fig. 2H).

In addition to COPII coat components, Sar1 was also more stably associated with membranes in Sedlin-depleted cells relative to control cells (Fig. 3A). Because Sar1 associates with membranes in its GTP-bound state, we tested the levels of Sar1-GTP in Sedlin-depleted cells. Using an antibody specific for Sar1-GTP, we observed higher levels of Sar1-GTP in Sedlin-depleted cells than in control cells (Fig. 3B and fig. S8). Slower COPII cycles and increased Sar1-GTP levels similar to those caused by Sedlin depletion were detected in Bet3/TRAPP-depleted cells (fig. S9), indicating that Sedlin acts to control the active state of Sar1 as a TRAPP component.

The increased Sar1-GTP levels observed after Sedlin depletion implied that ER exit of PC and VSV-G might be differentially sensitive to Sar1-GTP. We tested this hypothesis by evaluating the impact of microinjecting increasing amounts of the GTP-locked mutant of Sar1 ($His^{79} \rightarrow$ Gly; Sar1H79G) on the ER exit of PC and VSV-G. At a low level of Sar1H79G (0.1 mg/ml), ER exit of PC and VSV-G was not affected, whereas at an intermediate level (0.5 mg/ml), ER exit of PC, but not of VSV-G, was impaired (Fig. 3C and fig. S10). Higher levels of Sar1H79G (2.5 mg/ml) blocked exit of both cargoes, in agreement with previous reports (13).

A possible mechanism underlying the higher sensitivity of the ER export of PC to Sar1-GTP levels might involve the ability of Sar1-GTP to induce membrane constriction through its N-terminal amphipathic helix (14, 15). We tested our hypothesis by using electron tomography and 3D reconstruction to analyze the organization of ERES in SEDT fibroblasts. Relative to control cells, ERES in SEDT fibroblasts contained a high number of tubular buds that appeared as round profiles connected with each other as beads on a string because of multiple constrictions, too narrow to allow the incorporation of large cargoes (Fig. 3D). Thus, Sedlin depletion, by inducing an increase in Sar1-GTP that can constrict membranes, appears to lead to the formation of abnormal carriers that are inadequate to incorporate the large PC prefibrils.

We finally asked how Sedlin could affect the state of Sar1 and explored the possibility that the two proteins physically interact. Recombinant Sedlin bound both Sar1A and Sar1B (Fig. 4, A and B) preferentially in their GTP state (Fig. 4C). Among the TRAPP subunits tested, only Sedlin bound Sar1 (fig. S11). Because Sar1-GTP also interacts with Sec23 (16), we assessed whether Sedlin and Sec23 coexist in a complex with Sar1. Sedlin pulled down Sec23 only in the presence of Sar1 (Fig. 4D), indicating that Sedlin does not bind Sec23 directly and that the three proteins instead form a complex. TANGO1 did not affect the formation of the Sedlin–Sar1-GTP–Sec23 complex (Fig. 4D).

Taking advantage of the structural homology between Sedlin, a longin-domain protein (17), and SRX, the longin domain of SRα (one of the two SRP receptor subunits) (18) and between Sar1 and SRβ (the other SRP receptor subunit belonging to the ARF-Sar GTPase superfamily) (18), we modeled the Sedlin-Sar1 complex on the SRX-SRβ complex (18) and identified a putative Sedlin-Sar1 interaction surface (fig. S12). Mutating a residue [$His^{13} \rightarrow$ Ala (H13A); fig. S12] in this surface greatly impaired the Sar1-binding ability of Sedlin (Fig. 4E). Moreover, in contrast to wild-type Sedlin, SedlinH13A was not recruited by Sar1H79G in intact cells (Fig. 4F). Furthermore, relative to wild-type Sedlin, disease-associated Sedlin mutants exhibited a significantly lower affinity for Sar1 (Fig. 4G and fig. S11).

We have shown that Sedlin, acting in concert with TANGO1, is required for biogenesis of the megacarriers through which PC exits the ER. In our working hypothesis (fig. S13), the combined action of TANGO1 and Sedlin coordinates the stabilization of the inner COPII layer (through TANGO1) with efficient Sar1 cycling (through Sedlin) to prevent premature membrane constriction, thus allowing growth of nascent carriers and the incorporation of large PC prefibrils.

Our finding that Sedlin binds Sar1 adds a further layer to interactions between TRAPP and COPII, because Bet3 binds Sec23 (19), but only after Sar1 has been released from membranes and vesicles have detached from ER membranes (20). The Sedlin-Sar1 interaction precedes release of COPII vesicles and accelerates dissociation of Sar1 from membranes, thus allowing the next layer of interaction between COPII and TRAPP. TRAPP would then play a role in subsequent events such as Rab1 activation (7), thereby exhibiting the unique property of coupling the cycles of Sar1 and Rab1, two GTPases acting in series in ER-to-Golgi transport.

Supplementary Material

Refer to Web version on PubMed Central for supplementary material.

Acknowledgments

We thank A. Luini, G. D'Angelo, B. Franco, and G. Manco for insightful discussions; the Telethon EM Core Facility (project no. GTF08001) for the EM analysis; J. Gecz for the Sedlin cDNAs; R. Schekman for the Sar1A cDNA; W. Balch for the Sar1B and Sec23 cDNAs; and J. Kimura for the use of Rx chondrocytes. Supported by Telethon grants GSP08002 and GGP06166, AIRC grant IG 8623, and Programma Operativo Nazionale grant 01_00862 (M.A.D.M.), Telethon grant GGP07075 (C.W.), NIH grant NIH/AR053696 (B.M.V.), and grants from Plan Nacional (BFU2008-00414), Consolider (CSD2009-00016), Agència de Gestió d'Ajuts Universitaris i de Recerca (AGAUR) Grups de Recerca Emergents (SGR2009-1488; AGAUR–Catalan Government), the European Research Council (268692). (V.M.), and an AIRC fellowship (R.V.).

References and Notes

1. Zanetti G, Pahuja KB, Studer S, Shim S, Schekman R. Nat. Cell Biol. 2012; 14:20. [PubMed: 22193160]
2. Saito K, et al. Cell. 2009; 136:891. [PubMed: 19269366]
3. Malhotra V, Erlmann P. EMBO J. 2011; 30:3475. [PubMed: 21878990]
4. Wilson DG, et al. J. Cell Biol. 2011; 193:935. [PubMed: 21606205]
5. Gedeon AK, et al. Nat. Genet. 1999; 22:400. [PubMed: 10431248]
6. Tiller GE, et al. Am. J. Hum. Genet. 2001; 68:1398. [PubMed: 11326333]
7. Barrowman J, Bhandari D, Reinisch K, Ferro-Novick S. Nat. Rev. Mol. Cell Biol. 2010; 11:759. [PubMed: 20966969]
8. Bleasel JF, et al. J. Rheumatol. 1995; 22:255. [PubMed: 7738948]
9. Zankl A, et al. Am. J. Med. Genet. A. 2004; 129A:144. [PubMed: 15316962]
10. See supplementary materials on Science Online.
11. Mironov AA, et al. J. Cell Biol. 2001; 155:1225. [PubMed: 11756473]
12. Scrivens PJ, et al. Traffic. 2009; 10:724. [PubMed: 19416478]
13. Pepperkok R, Lowe M, Burke B, Kreis TE. J. Cell Sci. 1998; 111:1877. [PubMed: 9625750]
14. Long KR, et al. J. Cell Biol. 2010; 190:115. [PubMed: 20624903]
15. Bacia K, et al. Sci. Rep. 2011; 1:17. [PubMed: 22355536]
16. Bi X, Corpina RA, Goldberg J. Nature. 2002; 419:271. [PubMed: 12239560]
17. Jang SB, et al. J. Biol. Chem. 2002; 277:49863. [PubMed: 12361953]
18. Schlenker O, Hendricks A, Sinning I, Wild K. J. Biol. Chem. 2006; 281:8898. [PubMed: 16439358]

19. Cai H, et al. Nature. 2007; 445:941. [PubMed: 17287728]
20. Lord C, et al. Nature. 2011; 473:181. [PubMed: 21532587]

Europe PMC Funders Author Manuscripts

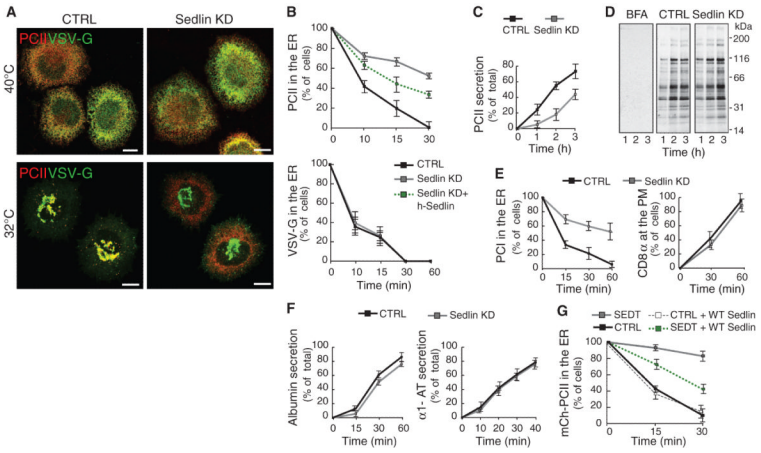

Fig. 1.

Sedlin is selectively required for the ER exit of procollagen. (**A**) PCII and VSV-G trafficking in mock (CTRL) or Sedlin KD Rx chondrocytes incubated for 3 hours at 40°C and then shifted to 32°C for 30 min. Scale bars, 10 μm. (**B**) Quantification of ER exit of PCII and VSV-G in cells treated as in (A) or in Sedlin KD cells expressing human Sedlin (Sedlin KD + h-Sedlin). Values are means ± SD ($N = 4$, $n = 200$ each time point). (**C**) PCII secretion from control or Sedlin KD Rx chondrocytes (10). Values are means ± SD ($N = 3$). (**D**) Total protein secretion in control or Sedlin KD Rx chondrocytes (10). As a negative control, mock cells were treated with brefeldin A (BFA; 10 μg/ml), a blocker of protein secretion. (**E**) Trafficking of PCI and CD8α in control or Sedlin KD fibroblasts (PM, plasma membrane). Values are means ± SD ($N = 4$, $n = 100$ each time point). (**F**) Secretion of albumin and α1-antitrypsin (α1-AT) in control and Sedlin KD HepG2 cells (10). Values are means ± SD ($N = 3$). (**G**) Quantification of mCherry-PCII ER exit in control or SEDT fibroblasts with or without coexpression of wild-type Sedlin. Cells were incubated for 3 hours at 40°C (time point 0) and then shifted to 32°C for 15 and 30 min. Values are means ± SD ($N = 3$, $n = 100$ each time point).

Europe PMC Funders Author Manuscripts

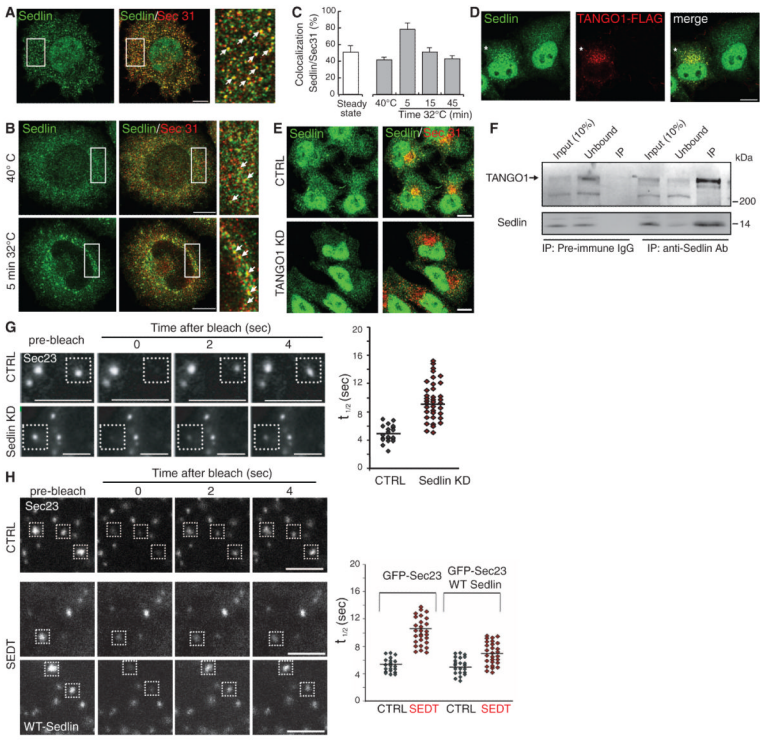

Fig. 2.

Sedlin is recruited by TANGO1 to the ERES and controls the COPII cycle. (**A**) Immunofluorescence of Sedlin and Sec31 in Rx chondrocytes at steady state. The rightmost panel is an enlargement of the boxed area; arrows indicate structures positive for both markers. (**B**) Immunofluorescence of Sedlin and Sec31 in Rx chondrocytes during a trafficking wave (incubation at 40°C for 3 hours and shift to 32°C for 5 min). The rightmost panels are enlargements of the boxed areas; arrows indicate structures positive for both markers. (**C**) Quantification of Sedlin and Sec31 colocalization. Values are means ± SD of colocalizing pixels as percentage of the total number of Sedlin pixels. (**D**) HeLa cells expressing FLAG-TANGO1 (asterisk) were immunostained with antibodies to FLAG and Sedlin. (**E**) Control or TANGO1 KD cells were immunostained for Sec31 and Sedlin. (**F**) Immunoprecipitates (IP) of pre-immune immunoglobulin G or antibody to Sedlin from HeLa cell lysates were analyzed by Western blot with antibodies to TANGO1 and Sedlin. (**G** and **H**) FRAP analysis of GFP-Sec23 at ERES in mock-treated (CTRL) and Sedlin KD fibroblasts (G) and in control and SEDT fibroblasts with or without wild-type Sedlin (H). Panels on the right in (G) and (H) show the FRAP $t_{1/2}$ of the indicated number of ERES. Scale bars, 10 μm [(A), (B), (D), (E)], 2 μm [(G), (H)].

Europe PMC Funders Author Manuscripts

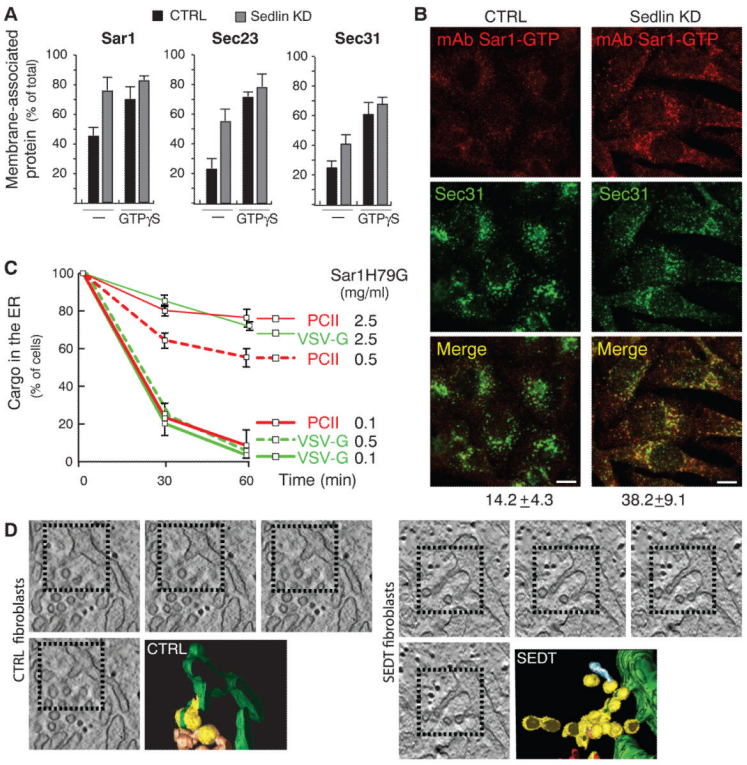

Fig. 3.

Sedlin depletion or mutation increases Sar1-GTP and induces membrane constrictions in nascent carriers at ERES. (**A**) Membrane association of Sar1, Sec23, and Sec31 evaluated as described in (10) in permeabilized control or Sedlin KD HeLa cells in the presence, where indicated, of 100 μM GTPγS. Values are means ± SD ($N = 4$, run in duplicate). (**B**) Control and Sedlin KD cells immunostained with antibodies to Sar1-GTP (10) and Sec31. Numbers below the Merge panels indicate the extent of colocalization of Sec31 with Sar1-GTP. Scale bars, 10 μm. (**C**) Quantification of the ER exit of PCII and VSV-G in Rx chondrocytes microinjected with Sar1H79G as indicated. Values are means ± SD ($N = 3$, $n = 200$ each time point). (**D**) Tomograms and 3D reconstruction of ERES in fibroblasts from healthy subjects (CTRL) and SEDT patients. COPII-coated buds (yellow), ER (green), and uncoated tubules (brownish) are highlighted. The incidence of buds with constrictions and constrictions per bud were higher in SEDT (54% and 3 to 6 constrictions per bud) than in controls (15% and 1 or 2 constrictions per bud).

Europe PMC Funders Author Manuscripts

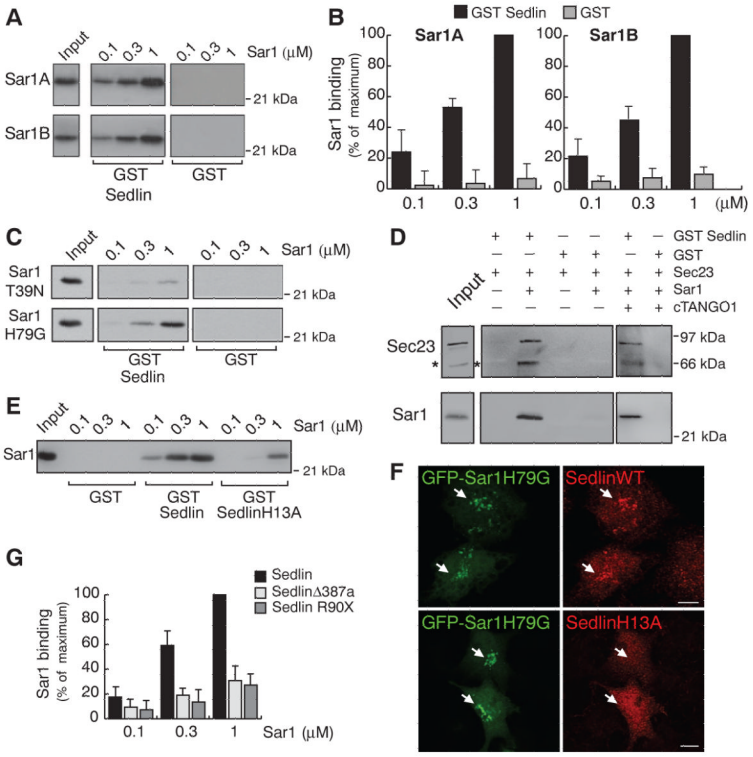

Fig. 4.

Sedlin binds Sar1-GTP. (**A**) Pull-down assays of Sar1A and Sar1B with 0.5 μM GST-Sedlin or GST. Sar1 input, 200 ng. (**B**) Quantification of Sedlin-Sar1 binding expressed as percent binding to 1 μM His-Sar1 (maximum). Values are means ± SD (N = 3). (**C**) As in (A) using His-tagged GDP- or GTP-restricted Sar1 mutant proteins (Sar1T39N and Sar1H79G, respectively). (**D**) Pull-down assays of GST-Sedlin or GST incubated with Sec23A (0.25 μM) in the absence or presence of 1 μM Sar1 and/or the cytosolic domain (amino acids 1211 to 1908) of TANGO1 (cTANGO1). Inputs: 10% of Sec23 and 2.5% of Sar1. Asterisks mark a degradation product of the His-Sec23 protein. (**E**) The same assay as in (A) using His-Sar1B with GST-Sedlin, GST-SedlinH13A, or GST. (**F**) GFP-Sar1H79G was coexpressed in HeLa cells with either wild-type Sedlin or SedlinH13A. Arrows indicate Sar1-positive areas. Scale bars, 10 μm. (**G**) Quantification of pull-down assays of Sar1 with GST, GST-Sedlin, or GST-tagged disease-associated Sedlin mutants (SedlinΔ387a and SedlinR90X), expressed as percentage of GST-Sedlin binding to 1 μM Sar1 (maximum). Values are means ± SD (N = 3).

Europe PMC Funders Author Manuscripts